Controlling cell shape on hydrogels using lift-off patterning

Jens Moeller[*a], Aleksandra K. Denisin[*a,b], Joo Yong Sim[a], Robin E. Wilson[a], Alexandre J.S. Ribeiro[a], Beth L. Pruitt[a,c,d]

* authors contributed equally

a. Department of Mechanical Engineering, Stanford University, Building 530
440 Escondido Mall, Stanford, CA 94305, USA.

b. Department of Bioengineering, Stanford University, 443 Via Ortega, Shriram Center, Room 119, Stanford, CA 94305-4125, USA.

c. Stanford Cardiovascular Institute, Stanford University, 265 Campus Drive
Stanford, CA 94305, USA.

d. Department of Molecular and Cellular Physiology, Stanford University School of Medicine, 279 Campus Drive, Beckman Center, Room B100A, Stanford, CA 94305-5345

Abstract

Polyacrylamide gels functionalized with extracellular matrix (ECM) proteins are commonly used as cell culture platforms to evaluate the combined effects of ECM composition, cell geometry and substrate rigidity on cell physiology. For this purpose, protein transfer onto the surface of polyacrylamide hydrogels must result in geometrically well-resolved micropatterns with homogeneous protein distribution. Yet the outcomes of micropatterning methods have not been pairwise evaluated against these criteria. We report a high fidelity photoresist lift-off patterning (LOP) method to pattern ECM proteins on polyacrylamide hydrogels ranging from 5 to 25 kPa. We directly compare the protein transfer efficiency and pattern geometrical accuracy of this protocol to the widely used microcontact printing (μCP) method. LOP achieves higher protein transfer efficiency, increases pattern accuracy, and reduces variability of these factors within arrays of patterns as it bypasses the drying and transfer steps of microcontact printing. We demonstrate that lift-off patterned hydrogels successfully control cell size and shape when we culture epithelial cells on these substrates.

Introduction

Cell culture substrates patterned with ECM are widely used to mimic the spatial organization and rigidity of the *in vivo* cell microenvironment *in vitro*. These cell culture platforms enable reductionist studies of the mechanobiology of healthy and diseased tissues under physiological-stiffness conditions (Théry, 2010). Specifically, polyacrylamide (PAAm) hydrogels are commonly used because these platforms can be functionalized with ECM and tuned in their mechanical properties to replicate different tissue stiffness ranging from ~0.1 kPa to ~40 kPa (Tse and Engler, 2010). Yet techniques for

patterning proteins on PAAm have lacked quantitative assessment, which is critical for developing and comparing protocols.

Broadly, two main strategies exist to pattern ECM on PAAm gels (reviewed in (Ribeiro et al., 2016)): i) selective activation of the gels for covalent attachment of proteins to activated regions (e.g. direct surface functionalization using UV-reactive sulfo-SANPAH crosslinkers (Tse and Engler, 2010) or polymerizing N-hydroxyacrylamide into the hydrogel surface (Grevesse et al., 2013)) and ii) co-polymerization of ECM proteins into the gels during gelation through direct contact of the acrylamide precursor mix with a protein-patterned coverslip. The first method, direct surface functionalization, uses expensive functionalization reagents and also depends on reagent quality and reaction time as the chemicals are unstable in aqueous media and in the presence of oxygen (Ribeiro et al., 2016). The method of co-polymerizing ECM proteins into the gel surface relies on patterning glass coverslips with protein and placing them in direct contact with the hydrogel during polymerization. Protein patterns on glass coverslips are often created by microcontact printing (μCP) using elastomeric 'stamps' (Alom Ruiz and Chen, 2007). Microcontact printing involves casting polydimethylsiloxane (PDMS) on microfabricated master structures created by photolithography to create stamps by replica molding (Qin et al., 2010). Most groups rely on microcontact printing since PDMS casting and contact printing protocols are straightforward once the master structures on silicon wafers are made (Rape et al., 2011; Tang et al., 2012; Zhang et al., 2013). However, μCP relies on the transfer of dried proteins from a deformable PDMS stamp to glass substrates and thus the accuracy, resolution, and pattern design are limited and critically depend on the PDMS stamp preparation and handling (Huang et al., 2005; Hui et al., 2002). To improve the accuracy, alternative protein patterning methods have been developed. For example, dip-pen nanolithography enables direct writing of proteins on flat, solid substrates with nanometer precision (Narui and Salaita, 2012). However, this method is serial and does not permit the functionalization of hydrogels. To overcome those challenges, protocols based on the selective oxidation of poly(l-lysine)-graft-poly(ethylene glycol) (PLL-g-PEG) layers by deep UV irradiation through a photomask or via projection lithography have been reported to pattern proteins on glass (Azioune et al., 2010; Strale et al., 2016). Those patterns can subsequently be transferred to a hydrogel (Vignaud et al., 2014) thereby decoupling pattern generation from hydrogel functionalization. Those methods however require either access to a collimated deep UV light source or a UV projection system, which are not readily available in most laboratories. Further, the PLL-g-PEG layer must either be dried prior to the UV irradiation, which requires a rehydration step prior to protein incubation (Azioune et al., 2010), or a photoinitiator must be added during the UV exposure step that has to be removed completely to re-establish the biopassive properties of the adlayer (Strale et al., 2016).

In this work, we present a photoresist lift-off patterning (LOP) method to control the shape of cells on PAAm hydrogels with high fidelity. Our method integrates advances in: i) contact photolithography and photoresist lift-off widely used in the semiconductor and microfabrication industry (Fredericks and Kotecha, 1986), ii) the molecular assembly and patterning of biopassive PLL-g-PEG coatings on glass(Anderegg et al., 2011; Falconnet et al., 2004; Moeller et al., 2013), and iii) the protein transfer from glass to PAAm hydrogels (Zhang et al., 2013).

We create protein-patterned glass coverslips by photoresist lift-off-assisted patterning of PLL-g-PEG and transfer the protein pattern to PAAm gel surfaces by co-polymerization. To demonstrate the utility of this approach, we successfully controlled the shape of MDCK cells cultured on patterned hydrogels. We benchmark the LOP technique to the widely used microcontact printing (μCP) across a range of physiologically relevant hydrogel stiffness (5 kPa, 10 kPa and 25 kPa) and analyze the pattern accuracy and transfer efficiency from the glass to the PAAm gel. We find that the LOP protocol improves both the pattern transfer efficiency and the pattern accuracy, thereby reducing the pattern variability and increasing the predictability of the engineered *in vitro* cell culture models.

Methods

Photoresist lift-off assisted patterning of ECM proteins (LOP)

ECM patterned glass coverslips were fabricated by photoresist lift-off (see process flow in Figure 1, full protocol in Supplemental Material). We first coated S1818 photoresist on coverslips (cleaned previously with 2% v/v Hellmanex in DI water (Hellma Analytics) overnight and rinsed 5 times in DI water) using standard contact photolithography (40-50 mJ/cm^2 at 365 nm, OAI Instruments) (Figure 1 i). We then incubated the photoresist-patterned substrates with 0.1 mg/ml (poly(l-lysine)-graft-poly(ethylene glycol) (PLL-g[3.5]-PEG (2kDa), SuSoS AG) for one hour. After photoresist lift-off in 1-methyl-2-pyrrolidone (NMP, Sigma 328634), we backfilled the PLL-g-PEG patterns with 100 μg/ml of Oregon Green-488 or Alexa Fluor 568-labeled gelatin solution in PBS pH 7.4 for 1 hour in the dark (Thermo Scientific, G13186, A10238) (Figure 1 ii-iv). The slides were washed thoroughly with DI water and excess liquid was removed by blotting on filter paper immediately prior to gel transfer. Gelatin, hydrolyzed collagen I, was chosen as model ECM protein to mimic the epithelial basement membrane because the Arg-Gly-Asp (RGD) sequence critical for cell adhesion, migration and proliferation is preserved (Zhu and Marchant, 2011). Gelatin, in contrast to collagen I, is also available commercially in a labeled form and can be labeled with standard protein labeling kits.

Microcontact printing of ECM proteins (μCP)

We prepared PDMS stamps by casting Sylgard 184 PDMS (10:1 base to curing agent) in a 9 μm deep mold microfabricated by standard photolithography using SU-8 negative resist (Qin et al., 2010). We

incubated the PDMS stamps (1 cm^2 squared stamps with 45 μm^2 patterns with 80 μm spacing) with 100 μg/ml fluorescently labeled gelatin solution for one hour in the dark. Following protein incubation, we aspirated excess protein solution and dried the stamps gently using low nitrogen gas flow. Prior to microcontact printing, we cleaned glass coverslips with 2% v/v Hellmanex solution in DI water for at least 30 minutes. We then rinsed the coverslips 5 times with DI water and dried them with compressed air prior to stamping. We put the PDMS stamps in contact with the cleaned coverslips for 5 minutes and removed the stamps by carefully forcing a tweezer between the coverslip and the edge of the stamp.

Preparation of ECM patterned polyacrylamide gels

We transferred the protein patterns from the glass coverslip to the surface of PAAm gel for both the LOP and μCP protocols by co-polymerization (Figure 1, v-vii). Polyacrylamide gels of varying stiffness were polymerized between the protein patterned glass coverslip and a silanized bottom coverslip. The bottom coverslip was silanized to ensure covalent bonding of gels to this bottom glass layer, following a method by Guo and colleagues (Guo and Wang, 2011). Briefly, 30 μL of working solution (3 μl bind-silane (3-methacryloxypropyl-trimethoxysilane, M6514 Sigma-Aldrich), 950 μL 95% ethanol, and 50 μL of glacial acetic acid) were applied to the coverslip, allowed to incubate for 5 min, and then rinsed with ethanol and dried in a desiccator.

Polyacrylamide gels of three different stiffness were used for experiments: 5 kPa, 10 kPa, and 25 kPa as determined by Tse and Engler (Tse and Engler, 2010). MilliQ water, acrylamide (0.5 g/mL stock, Sigma-Aldrich, 01696 FLUKA), and bis-acrylamide (0.025 g/mL stock, Sigma-Aldrich, 146072) were combined to yield 5% w/v acrylamide and 0.15% w/v bis-acrylamide for 5 kPa gels, 10% w/v acrylamide and 0.1% w/v bis-acrylamide for 10 kPa gels, and 10% w/v acrylamide and 0.25% w/v bis-acrylamide for 25 kPa gels. The precursor solution was degassed in a vacuum desiccator for 1 hr. To initiate gelation, 5 μL of 10% w/v ammonium persulfate (APS, Sigma-Aldrich, A9164) was added to ~995 μL of gel precursor solution followed by 0.5 μL of N,N,N′,N′-Tetramethylethylenediamine accelerator (TEMED, Sigma-Aldrich, 411019). The solutions were mixed by gentle pipetting, 50 μL of the solution was dispersed on the activated coverslip, and the protein-functionalized coverslip was placed on top (Figure 1 v). Gels were left undisturbed at room temperature for 30 minutes to polymerize. After polymerization, the gels were immersed in PBS for at least 1 hour and the glass coverslip was removed from the top of the gels (Figure 1 vi).

Analysis of Pattern Transfer Efficiency

To assess the protein transfer efficiency from the patterned glass coverslip onto the PAAm gel, we imaged the coverslips before transfer and the PAAm gel surface after gelation and coverslip removal using the same microscope image acquisition parameters. All acquired images were processed by ImageJ (http://rsb.info.nih.gov/ij/). We analyzed 150 individual patterned features by measuring the

difference between the same feature on the coverslip before and after transfer, using the cvMatch_Template ImageJ plugin (Tseng et al., 2011). The average background signal was determined outside the protein pattern and subtracted for each image. We measured the average pixel intensity within a region of interest defined as our theoretical patterning shape and calculated the transfer efficiency as the average intensity of the protein pattern on the gel image divided by the average intensity of the pattern on the coverslip.

Analysis of the Geometric Accuracy of Protein Patterning

To compare the accuracy of patterns generated by lift-off and microcontact printing, we calculated the cross-correlation coefficient between the theoretical pattern shape and the binarized patterned features using the *corr2* function in Matlab (R2014b, Mathworks). The binarized pattern stacks were created with ImageJ by de-noising the images using the built-in despeckle function followed by automated binarization of each pattern using Otsu thresholding.

Cell culture

Madin-Darby Canine Kidney (MDCK) type II G cells were transfected with LifeAct-GFP (ibidi, 60101) using the Amaxa Biosystem Nucleofector II system and transfection kit (Lonza, VCA-1005). The LifeAct-GFP MDCK cells were maintained in low glucose DMEM (Invitrogen, 11885) containing 1 g/l sodium bicarbonate, 1% Penicillin-Streptomycin (PenStrep, ThermoFisher, 15140122), 0.5 mg/ml G418 selection reagent (Sigma-Aldrich, G418-RO Roche), and supplemented with 10% (vol/vol) fetal bovine serum (FBS). 25 kPa PAAm gels patterned with 100 µg/ml collagen I (Gibco, A1048301) mixed with 20 µg/ml Alexa Fluor 568 labeled gelatin were cast into Mattek dishes (14 mm glass, Mattek P35G-0.170-14-C). MDCK cells were trypsinized and seeded on the PAAm gels for 16 hours before imaging experiments. Prior to imaging, the media was replaced to low glucose DMEM with no phenol red (ThermoFisher, 11054001) and supplemented with 1% PenStrep, 10% FBS, and 25 mM HEPES buffer. Cells were imaged on a Leica DMI3000B microscope with heated incubation unit at 5 minute intervals using a 40x air objective.

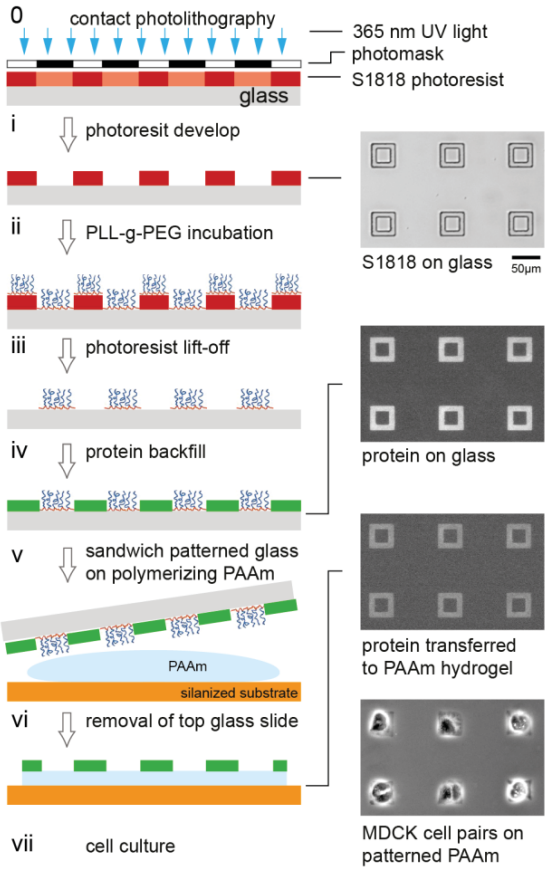

Figure 1 LOP fabrication of protein patterns on polyacrylamide gels.
(i) Photoresist patterns are fabricated by standard contact photolithography on glass coverslips. Inset at right shows array of S1818 photoresist features after development. (ii) Unspecific protein adhesion to the resist-patterned coverslip is blocked by incubating with biopassive PLL-g[3.5]-PEG(2kDa) copolymer. (iii-iv) Following photoresist lift-off, the resulting PLL-g-PEG pattern is backfilled with the ECM protein of interest. Inset at right shows a fluorescence micrograph of a labeled protein on glass after backfill. (v) To transfer the protein pattern to the PAAm gel, the gel is polymerized between the protein patterned glass coverslip and a silanized coverslip. (vi) After gel polymerization, the top coverslip is removed from the PAAm gel. Inset at right shows a fluorescence micrograph of a labeled protein transferred to a PAAm gel. (vii) Inset at right shows pairs of epithelial cells on the patterned PAAm gel assuming the geometry of the protein functionalized regions.

Results

We compare the LOP and μCP methods by analyzing the efficiency of protein transfer from the surface of coverslips onto the surface of PAAm gels (Figure 2) and the geometrical accuracy of the patterns (Figure 3). We use a square 'frame' pattern shape to specifically compare how both protocols resolve corners and edges of a complex shape. We show pattern arrays of glass and PAAm samples normalized for contrast to aid visual comparison of the transfer efficiency for lift-off and microcontact printing techniques in Figure 2A and 2B.

Protein patterns created by the LOP method are transferred more efficiently from the coverslips to gels for all gel stiffness we tested (Figure 2C). We find significant differences in transfer efficiency between LOP and µCP when comparing both protocols at each stiffness (p-value < 2.2E-16 for the 5 kPa, 10 kPa, and 25 kPa PAAm gel samples). However, the protein transfer efficiency in both methods is considerably lower for 5 kPa when compared to 10 kPa and 25 kPa PAAm samples. To explain this observation, we analyzed and compared the size properties of gelatin and polyacrylamide gel formulations used in this study to those commonly used in mechanobiology and electrophoresis (see Supplemental Information). The 10 kPa and 25 kPa gel formulations we use contain 10% total polymer which is twice that of the 5 kPa gel formulation (5%). Due to the lower total polymer content, we hypothesize that fewer sites are available for protein integration during polymerization in the 5 kPa gels. This effect is independent of the protein patterning technique and thus can be a limiting factor for the protein functionalization of soft polyacrylamide gels.

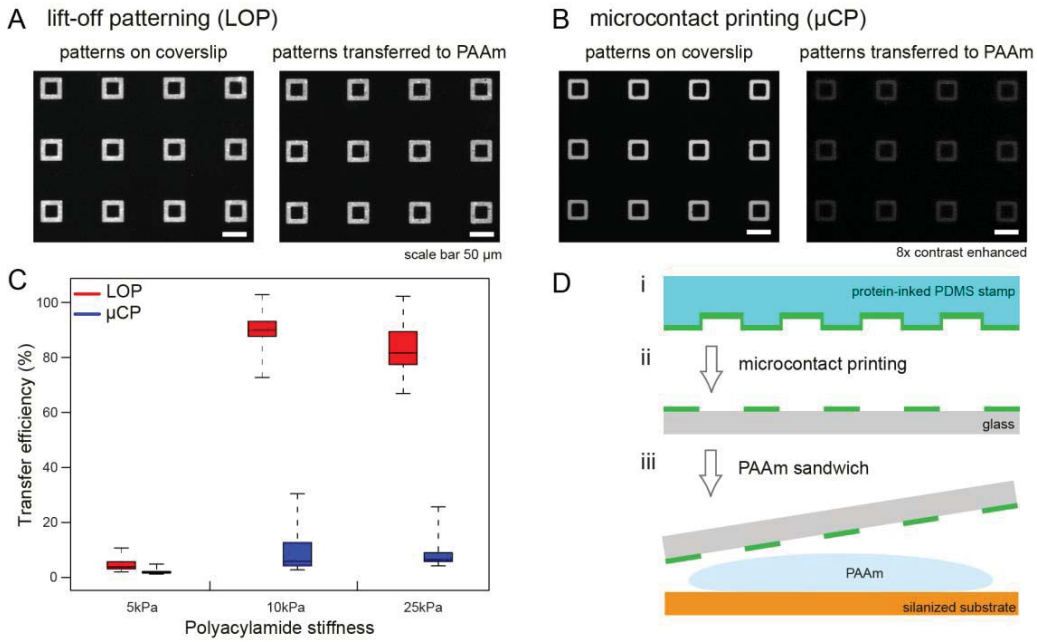

Figure 2 Quantification of protein transfer efficiency to PAAm gels of varying stiffness. (A,B) Arrays of 45 µm^2 square protein patterns on 25 kPa PAAm gels created by LOP and µCP before and after transfer to gel surface. (C) Quantification of protein transfer efficiency from glass coverslips to PAAm gel of varying stiffness. Differences between LOP and µCP for each stiffness are statistically significant (p-value < 2.2E-16, Mann-Whitney-Wilcoxon test). Substantially more protein is transferred from patterns created by photoresist lift-off. Data are represented as box plots. The median, 1st and 3rd quartile, and minimum and maximum values are shown, n = 150 for each method and stiffness shown. (D) Overview of µCP method to pattern proteins on PAAm gels.

To evaluate the accuracy of the features transferred to PAAm gels, we compare the corners of the square frame patterns for both protocols (Figure 3A) and show the difference between the actual and

theoretical shape (Figure 3B). Protein patterns created by LOP exhibit greater definition in the edges and corners (inner, outer) and recapitulate the theoretical pattern shape on the photomask with higher fidelity than protein patterns created by µCP. The LOP photolithography step results in higher spatial resolution than µCP because the LOP photoresist layer is thin (2 µm) compared to the thicker photoresist layer used as master structure for fabricating the PDMS stamps (9 µm). Thus, the starting features for µCP exhibit curved corners (Supplemental Figure 1) which leads to a decrease in pattern accuracy. We quantitatively compared plot profile scans across 150 patterns created by both methods to the theoretical pattern shape (Figure 3D; similar to methods by Vignaud and colleagues (Vignaud et al., 2014)). Cross-correlation analysis of the fabricated patterns with the theoretical shape quantitatively shows that LOP results in patterns that more accurately recapitulate the theoretical shape. Correlation coefficients are as follows (n = 150 patterns; mean +/- standard deviation): µCP (5, 10, 25 kPa): 0.84±0.05; 0.87±0.02; 0.89±0.02; LOP (5, 10, 25 kPa): 0.91±0.04; 0.94±0.02; 0.93±0.01).

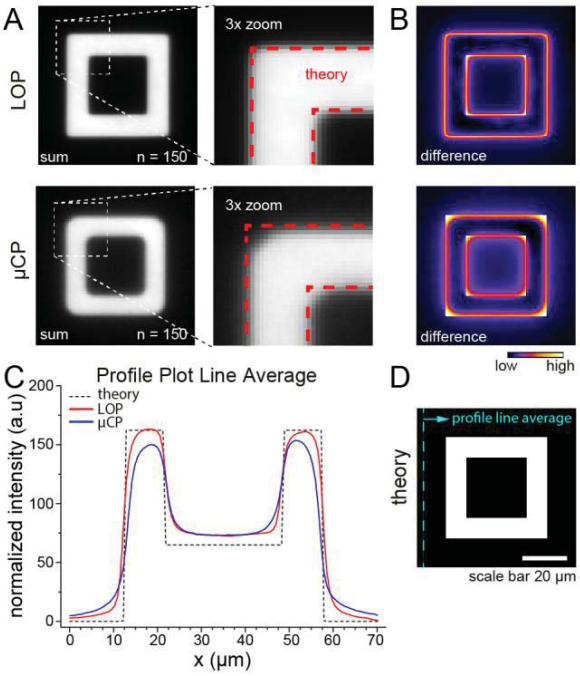

Figure 3 Comparison of pattern accuracy between LOP and µCP methods.
(A) Normalized sum images of 150 protein patterns created by LOP and µCP on 25 kPa gels are compared to the theoretical pattern shape. (B) Error images calculated by subtracting the normalized sum images from the theoretical pattern mask. Edges and corners are resolved substantially better in patterns created by LOP. (C) Plot profile scan across 150 patterns created by µCP and LOP methods compared to the (D) theoretical pattern shape shows that LOP results in patterns of greater accuracy than µCP.

We demonstrate that single cells as well as pairs of cells only attach to ECM patterned areas of the PAAm gels functionalized with coverslips patterned using the LOP method (Figure 4A,B; SI Movies 1, 2). Areas between patterns exhibit anti-adhesive properties and prevent cells from binding to the gel outside the protein features. To test if the cytoskeletal architecture and remodeling are different for cells attached to patterns created by LOP or µCP, we followed the actin dynamics of LifeAct-GFP transfected MDCK cells using live cell fluorescence microscopy. Consistent with previous literature reports (Tseng et al., 2012), we found that cell doublets on the frame patterns rotated around each other (Figure 4B,D; SI Movies 2, 4). While this was observed independent of the patterning method used, the cell edges were more clearly defined for cells adhering to patterns created by LOP than gels patterned by µCP (Figure 5), which was consistent with the higher pattern accuracy.

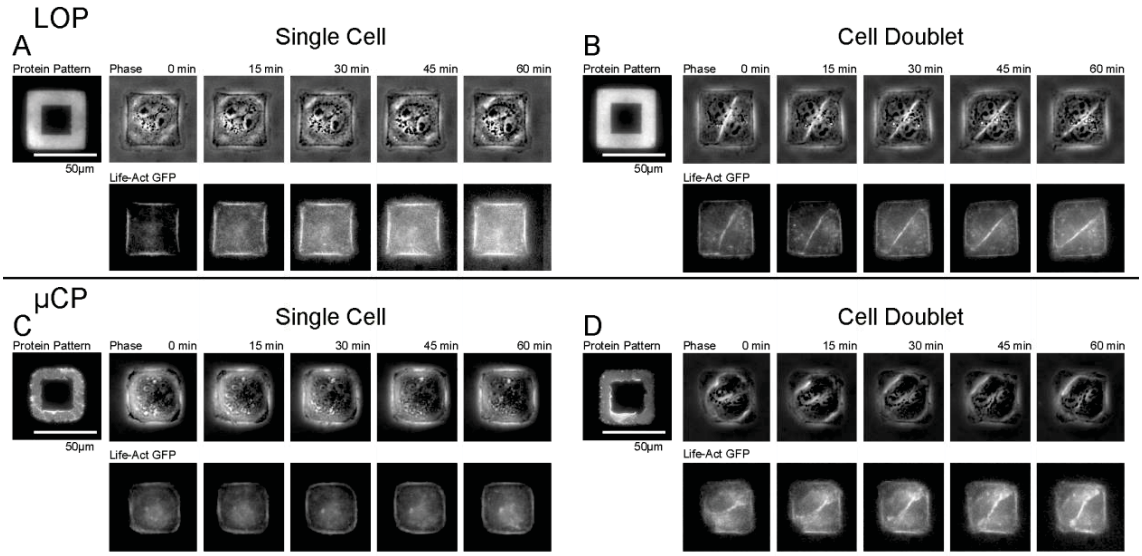

Figure 4 Analysis of actin dynamics in epithelial cells on LOP and µCP patterned gels.
Time-lapse acquisitions of MDCK cells transfected with the Lifeact-GFP actin marker grown on 25 kPa PAAm gels showed similar intracellular actin structures on LOP (A,B) and µCP (C,D) protein patterns. Cell doublets rotated around each other on the patterns for both techniques (B,D).

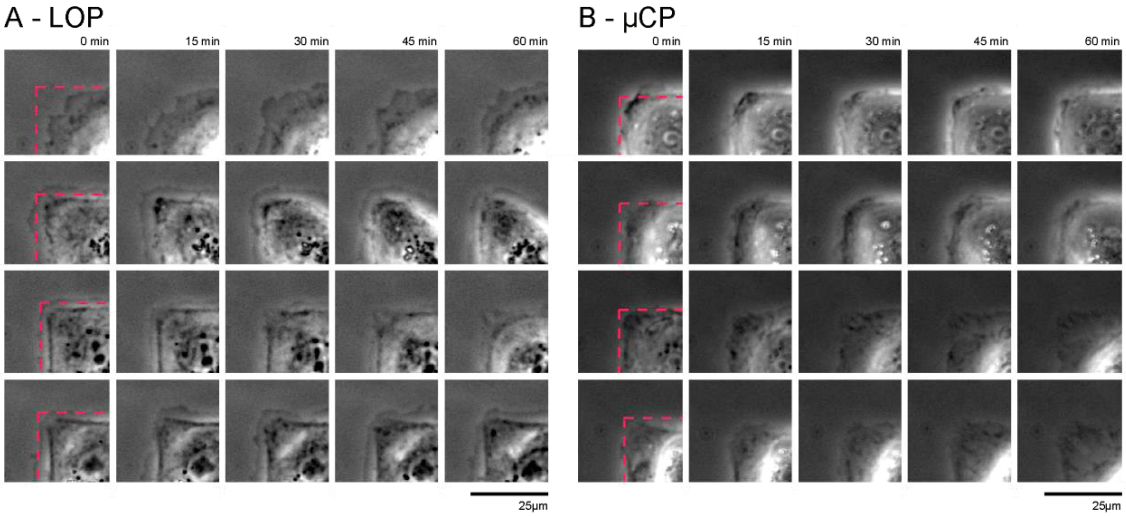

Figure 5 Cell filopodia are more pronounced on LOP than on µCP patterned substrates. Time lapse imaging of 4 representative MDCK cells on 25 kPa PAAm gels patterned by LOP (A) and µCP (B) shows more pronounced lamellipodia in cells on LOP substrates. MDCK cells on substrates produced by LOP also have a better-defined shape which more accurately follows the protein pattern border (shown in dotted red).

Discussion

In this work, we introduce a photoresist lift-off patterning (LOP) technique to pattern ECM proteins on polyacrylamide hydrogels to control the shape of cells with high fidelity and compare it with the widely used microcontact printing protocol (µCP). We found the LOP method to be more efficient and accurate in reproducing complex micrometer-sized patterns (Figure 2,3). LOP relies on the molecular assembly of the biopassive PLL-g-PEG copolymer on the photoresist structures and thus the accuracy of this method primarily depends on the resolution of the photolithography step (Figure 1). µCP, in contrast, involves multiple critical steps that affect the transfer efficiency and accuracy: the drying of proteins on the PDMS stamps, the transfer of the protein from the flexible stamp to the coverslip, and the interaction between the proteins and the glass surface. Further, LOP enables the design and fabrication of arbitrary pattern geometry and spatial organization (e.g., large pattern-to-pattern distance) as LOP circumvents the need to maintain specific height-width ratios in PDMS stamps to keep the elastomeric structures from collapsing during µCP (Delamarche et al., 1997; Hui et al., 2002). Ultimately, the spatial resolution that can be achieved with the LOP is determined by the photolithography step (Figure 1). The ideal spatial resolution (R) can be estimated using the following relation between the exposure wavelength (λ) and the photoresist thickness (z) in contact photolithography (Madou, 2011):

$$R = 1.5 * \sqrt{\lambda \frac{z}{2}}$$

As a proof-of-concept, we seeded MDCK epithelial cells on frame patterns (Figure 4,5; SI Movies 1 - 4). Independent of the patterning method, cells only attached to the protein patterns due to the non-adhesive properties of the polyacrylamide gel surface in between patterns. An open question for patterns created by LOP is whether the PLL-g-PEG blocking agent on the glass coverslips is transferred to the PAAm gel. We are not able to trace fluorescently labeled PLL-g-PEG molecules in the gel samples but individual PEG chains have been shown to polymerize into the backbone of polyacrylamide when added in bulk to the precursor solution (Pantar, 1986). The interactions of PLL-g-PEG copolymer and polyacrylamide during gel polymerization are unclear. Regardless of PLL-g-PEG transfer to the PAAm surface, LOP results in functionalized PAAm gels with non-adhesive regions between protein patterns. We noted that removing the glass coverslips from polymerized gels was easier for samples created by LOP than for μCP (step shown in Figure 1, vi) and we hypothesize that this effect could be due to the high water content of the PLL-g-PEG layer (Pasche et al., 2005).

In summary, our LOP method facilitates advanced cell culture techniques that require precise patterning of single or multiple cells into a variety of shapes on substrates of varied stiffness. High pattern accuracy and defined ECM density within the protein patterns is essential to compare cell phenotypes on different patterns and reduce the systematic error of pooled measurements. This is of particular importance for studies focusing on complex, multivariate cell-ECM signaling pathways and the cytoskeletal response to different cell geometries and substrate stiffness (Tseng and Di Carlo, 2014). Overall, local ECM density, cell shape, and substrate stiffness have been shown to regulate the structural organization of focal adhesion complexes (Balaban et al., 2001; Cavalcanti-Adam et al., 2007), the force balance between cell-cell and cell-ECM adhesions (Sim et al., 2015), the nuclear lamina (Ihalainen et al., 2015), mesenchymal stem cell stiffness (Tee et al., 2011), stem cell fate (Lee et al., 2013; Trappmann et al., 2012), and the contractile properties of cardiomyocytes (Ribeiro et al., 2015).

Acknowledgements

The authors would like to thank Pruitt lab members for useful discussion of results. This project was supported in part by the National Science Foundation (NSF-1136790, EFRI-MIKS), National Institutes of Health (NIH- R01EB006745, NIH-1R21HL13099301). The authors are grateful for graduate and post-doctoral research fellowships from the National Science Foundation, ILJU Foundation, Stanford BioX, Stanford Office of the Vice Provost for Graduate Education, American Heart Association, and Stanford Graduate Fellowship.

References

Alom Ruiz, S., and Chen, C.S. (2007). Microcontact printing: A tool to pattern. Soft Matter *3*, 168-177.

Anderegg, F., Geblinger, D., Horvath, P., Charnley, M., Textor, M., Addadi, L., and Geiger, B. (2011). Substrate adhesion regulates sealing zone architecture and dynamics in cultured osteoclasts. PLoS One *6*, e28583.

Azioune, A., Carpi, N., Tseng, Q., Théry, M., and Piel, M. (2010). Protein Micropatterns. A Direct Printing Protocol Using Deep UVs. Methods Cell Biol *97*, 133-146.

Balaban, N.Q., Schwarz, U.S., Riveline, D., Goichberg, P., Tzur, G., Sabanay, I., Mahalu, D., Safran, S., Bershadsky, A., Addadi, L., *et al.* (2001). Force and focal adhesion assembly: a close relationship studied using elastic micropatterned substrates. Nat Cell Biol *3*, 466-472.

Cavalcanti-Adam, E.A., Volberg, T., Micoulet, A., Kessler, H., Geiger, B., and Spatz, J.P. (2007). Cell Spreading and Focal Adhesion Dynamics Are Regulated by Spacing of Integrin Ligands. Biophys J *92*, 2964-2974.

Delamarche, E., Schmid, H., Michel, B., and Biebuyck, H.A. (1997). Stability of molded polydimethylsiloxane microstructures. Adv Mater *9*, 741-746.

Falconnet, D., Koenig, A., Assi, F., and Textor, M. (2004). A Combined Photolithographic and Molecular-Assembly Approach to Produce Functional Micropatterns for Applications in the Biosciences. Adv Funct Mater *14*, 749-756.

Fredericks, E.C., and Kotecha, H.N. (1986). Photoresist lift-off process for fabricating semiconductor devices. (United States Patent).

Grevesse, T., Versaevel, M., Circelli, G., Desprez, S., and Gabriele, S. (2013). A simple route to functionalize polyacrylamide hydrogels for the independent tuning of mechanotransduction cues. Lab Chip *13*, 777-780.

Guo, W.-H., and Wang, Y.-l. (2011). Micropatterning cell-substrate adhesions using linear polyacrylamide as the blocking agent. Cold Spring Harb Protoc *2011*, prot5582.

Huang, Y.Y., Zhou, W., Hsia, K.J., Menard, E., Park, J.-U., Rogers, J.A., and Alleyne, A.G. (2005). Stamp Collapse in Soft Lithography. Langmuir *21*, 8058-8068.

Hui, C.Y., Jagota, A., Lin, Y.Y., and Kramer, E.J. (2002). Constraints on microcontact printing imposed by stamp deformation. Langmuir *18*, 1394-1407.

Ihalainen, T.O., Aires, L., Herzog, F.A., Schwartlander, R., Moeller, J., and Vogel, V. (2015). Differential basal-to-apical accessibility of lamin A/C epitopes in the nuclear lamina regulated by changes in cytoskeletal tension. Nat Mater *14*, 1252-1261.

Lee, J., Abdeen, A.A., Zhang, D., and Kilian, K.A. (2013). Directing stem cell fate on hydrogel substrates by controlling cell geometry, matrix mechanics and adhesion ligand composition. Biomaterials *34*, 8140-8148.

Madou, M.J. (2011). Manufacturing Techniques for Microfabrication and Nanotechnology, Vol 2, 3 edn (CRC Press).

Moeller, J., Emge, P., Avalos Vizcarra, I., Kollmannsberger, P., and Vogel, V. (2013). Bacterial filamentation accelerates colonization of adhesive spots embedded in biopassive surfaces. New J Phys *15*, 125016.

Narui, Y., and Salaita, K.S. (2012). Dip-pen nanolithography of optically transparent cationic polymers to manipulate spatial organization of proteolipid membranes. Chem Sci *3*, 794-799.

Pantar, A.V. (1986). The polymerization of acrylamide in the presence of poly(ethylene glycol) II. European Polymer Journal *22*, 939-942.

Pasche, S., Vöros, J., Griesser, H.J., Spencer, N.D., and Textor, M. (2005). Effects of ionic strength and surface charge on protein adsorption at PEGylated surfaces. J Phys Chem B *109*, 17545-17552.

Qin, D., Xia, Y., and Whitesides, G.M. (2010). Soft lithography for micro- and nanoscale patterning. Nat Protoc *5*, 491-502.

Rape, A.D., Guo, W.-H., and Wang, Y.-l. (2011). The regulation of traction force in relation to cell shape and focal adhesions. Biomaterials *32*, 2043-2051.

Ribeiro, A.J.S., Ang, Y.-S., Fu, J.-D., Rivas, R.N., Mohamed, T.M.A., Higgs, G.C., Srivastava, D., and Pruitt, B.L. (2015). Contractility of single cardiomyocytes differentiated from pluripotent stem cells depends on physiological shape and substrate stiffness. Proc Natl Acad Sci U S A.

Ribeiro, A.J.S., Denisin, A.K., Wilson, R.E., and Pruitt, B.L. (2016). For whom the cells pull: Hydrogel and micropost devices for measuring traction forces. Methods *94*, 51-64.

Sim, J.Y., Moeller, J., Hart, K.C., Ramallo, D., Vogel, V., Dunn, A.R., Nelson, W.J., and Pruitt, B.L. (2015). Spatial Distribution of Cell-Cell and Cell-ECM Adhesions Regulates Force Balance while Maintaining E-cadherin Molecular Tension in Cell Pairs. Mol Biol Cell *26*, 2456-2465.

Strale, P.-O., Azioune, A., Bugnicourt, G., Lecomte, Y., Chahid, M., and Studer, V. (2016). Multiprotein Printing by Light-Induced Molecular Adsorption. Adv Mater Weinheim *28*, 2024-2029.

Tang, X., Ali, M.Y., and Saif, M.T.A. (2012). A Novel Technique for Micro-patterning Proteins and Cells on Polyacrylamide Gels. Soft Matter *8*, 7197-7206.

Tee, S.-Y., Fu, J., Chen, C.S., and Janmey, P.A. (2011). Cell Shape and Substrate Rigidity Both Regulate Cell Stiffness. Biophys J *100*, L25-L27.

Théry, M. (2010). Micropatterning as a tool to decipher cell morphogenesis and functions. J Cell Sci *123*, 4201-4213.

Trappmann, B., Gautrot, J.E., Connelly, J.T., Strange, D.G.T., Li, Y., Oyen, M.L., Cohen Stuart, M.A., Boehm, H., Li, B., Vogel, V., *et al.* (2012). Extracellular-matrix tethering regulates stem-cell fate. Nat Mater *11*, 642-649.

Tse, J.R., and Engler, A.J. (2010). Preparation of hydrogel substrates with tunable mechanical properties. Curr Protoc Cell Biol *47*, Unit 10.16.

Tseng, P., and Di Carlo, D. (2014). Substrates with Patterned Extracellular Matrix and Subcellular Stiffness Gradients Reveal Local Biomechanical Responses. Adv Mater Weinheim *26*, 1242-1247.

Tseng, Q., Duchemin-Pelletier, E., Deshiere, A., Balland, M., Guillou, H., Filhol, O., and Théry, M. (2012). Spatial organization of the extracellular matrix regulates cell–cell junction positioning. Proc Natl Acad Sci U S A *109*, 1506-1511.

Tseng, Q., Wang, I., Duchemin-Pelletier, E., Azioune, A., Carpi, N., Gao, J., Filhol, O., Piel, M., Théry, M., and Balland, M. (2011). A new micropatterning method of soft substrates reveals that different tumorigenic signals can promote or reduce cell contraction levels. Lab Chip *11*, 2231.

Vignaud, T., Ennomani, H., and Théry, M. (2014). Polyacrylamide Hydrogel Micropatterning. (Elsevier), pp. 93-116.

Zhang, J., Guo, W.-H., Rape, A., and Wang, Y.-l. (2013). Micropatterning Cell Adhesion on Polyacrylamide Hydrogels. (Totowa, NJ: Humana Press), pp. 147-156.

Zhu, J., and Marchant, R.E. (2011). Design properties of hydrogel tissue-engineering scaffolds. Expert Rev Med Devices *8*, 607-626.

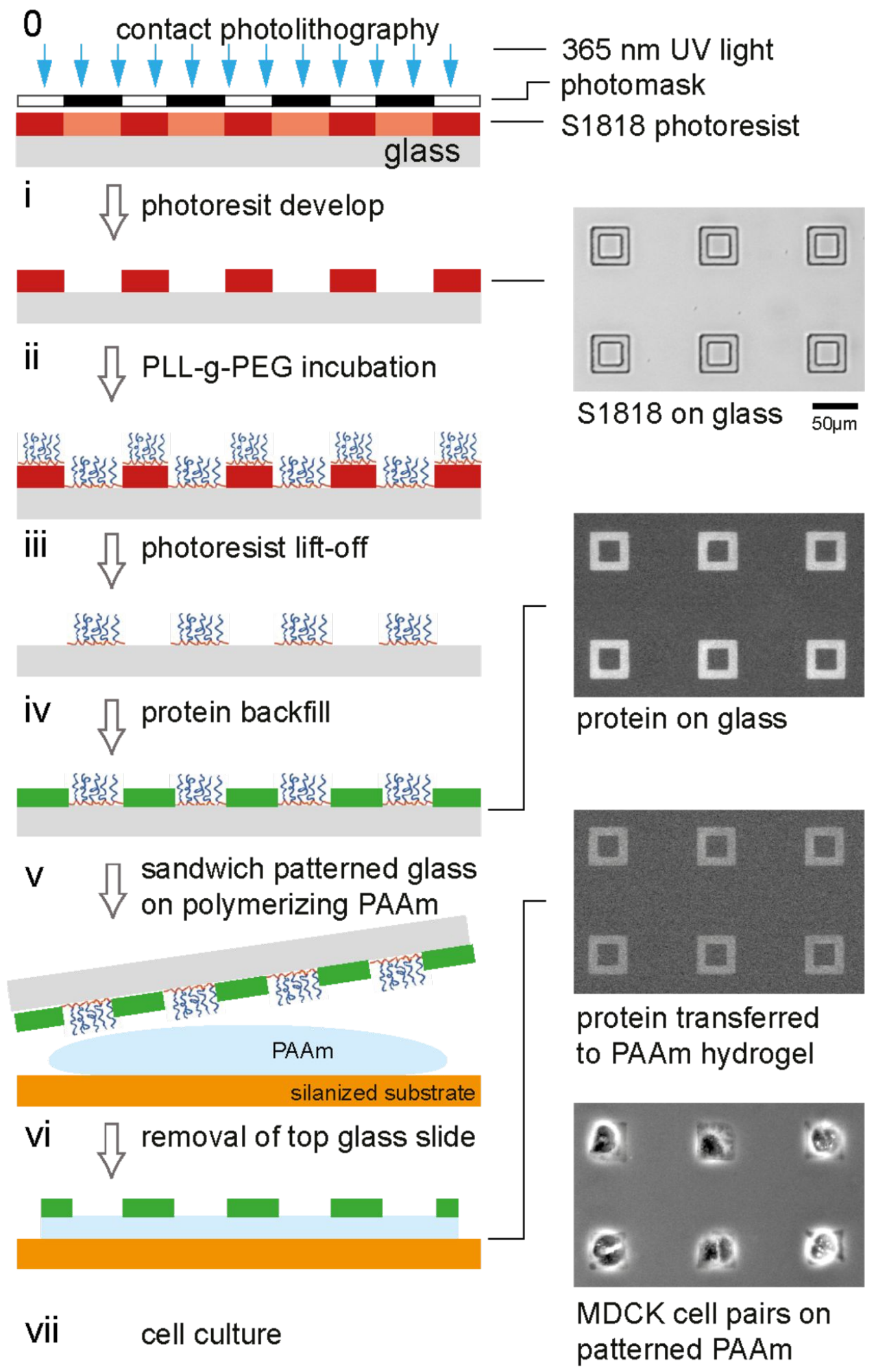
0
contact photolithography
365 nm UV light
photomask
S1818 photoresist
glass
i
photoresit develop
S1818 on glass
50μm
ii
PLL-g-PEG incubation
iii
photoresist lift-off
iv
protein backfill
protein on glass
v
sandwich patterned glass
on polymerizing PAAm
PAAm
silanized substrate
protein transferred
to PAAm hydrogel
vi
removal of top glass slide
vii
cell culture
MDCK cell pairs on
patterned PAAm

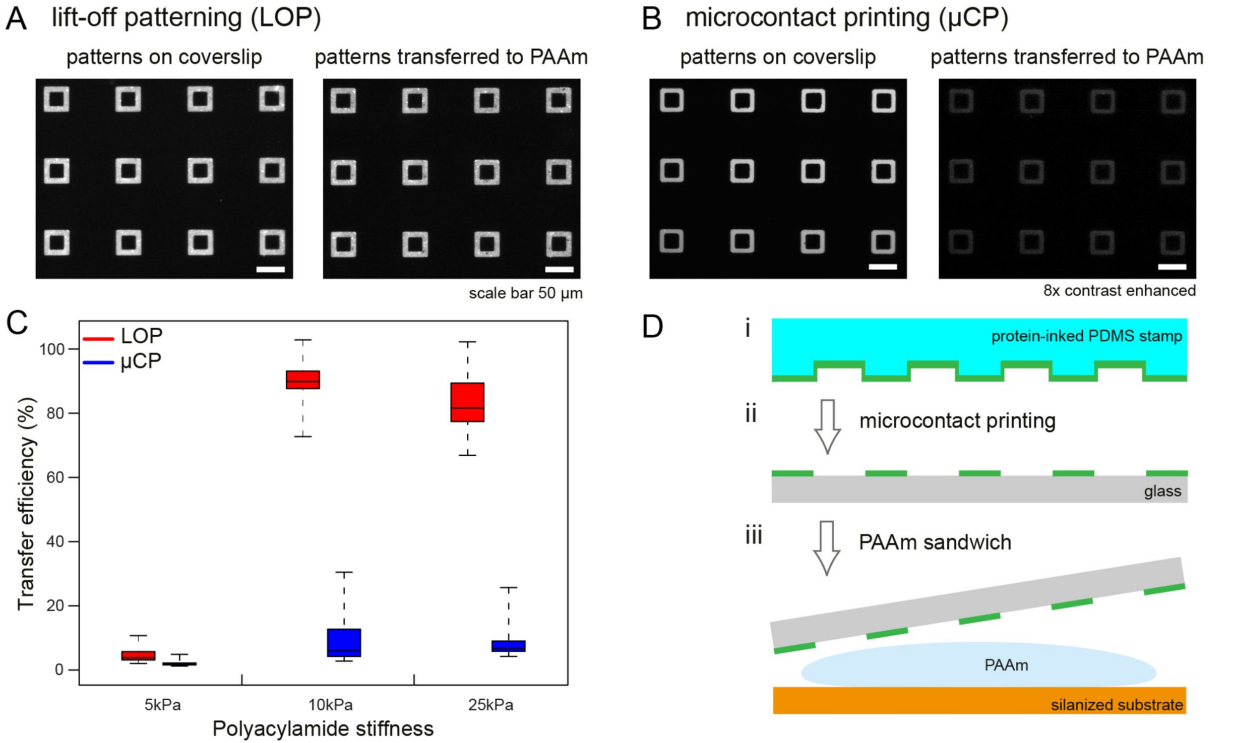
A
lift-off patterning (LOP)
patterns on coverslip
patterns transferred to PAAm
scale bar 50 µm
B
microcontact printing (µCP)
patterns on coverslip
patterns transferred to PAAm
8x contrast enhanced
C
LOP
µCP
Transfer efficiency (%)
100
80
60
40
20
0
5kPa
10kPa
25kPa
Polyacylamide stiffness
D
i
protein-inked PDMS stamp
ii
microcontact printing
glass
iii
PAAm sandwich
PAAm
silanized substrate

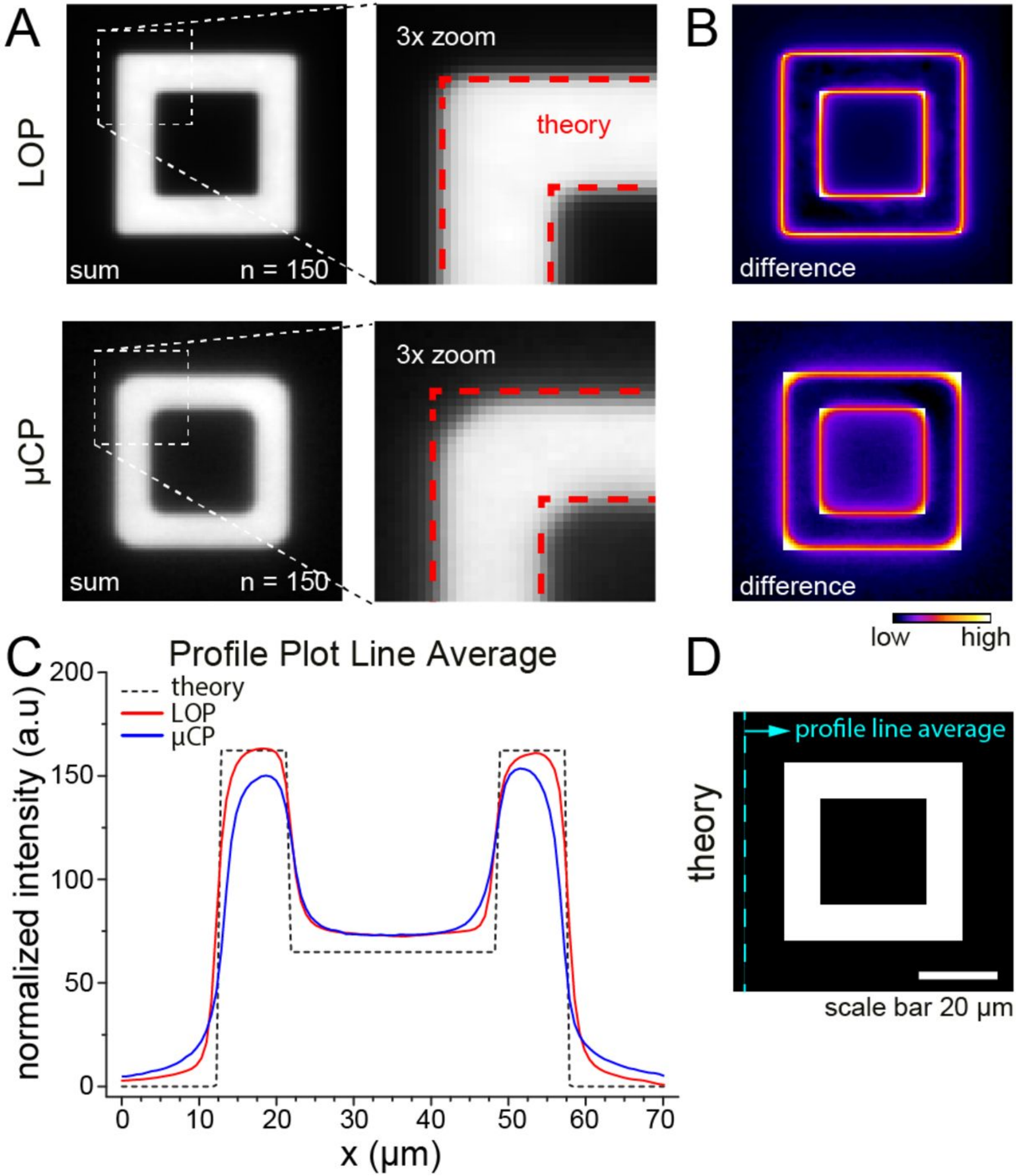
A
LOP
sum
n = 150
3x zoom
theory
B
difference
μCP
sum
n = 150
3x zoom
difference
low
high
C
Profile Plot Line Average
theory
LOP
μCP
normalized intensity (a.u)
200
150
100
50
0
0
10
20
30
40
50
60
70
x (μm)
D
theory
profile line average
scale bar 20 μm

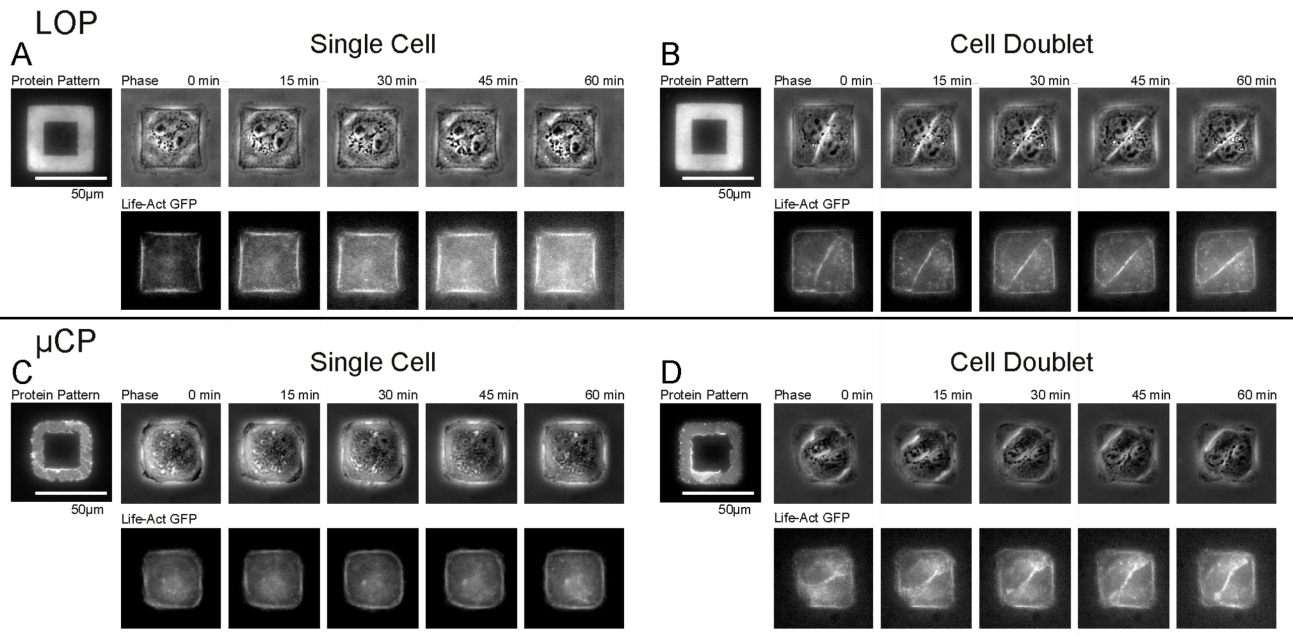
LOP
A
Single Cell
Protein Pattern
Phase
0 min
15 min
30 min
45 min
60 min
50µm
Life-Act GFP
B
Cell Doublet
Protein Pattern
Phase
0 min
15 min
30 min
45 min
60 min
50µm
Life-Act GFP
µCP
C
Single Cell
Protein Pattern
Phase
0 min
15 min
30 min
45 min
60 min
50µm
Life-Act GFP
D
Cell Doublet
Protein Pattern
Phase
0 min
15 min
30 min
45 min
60 min
50µm
Life-Act GFP

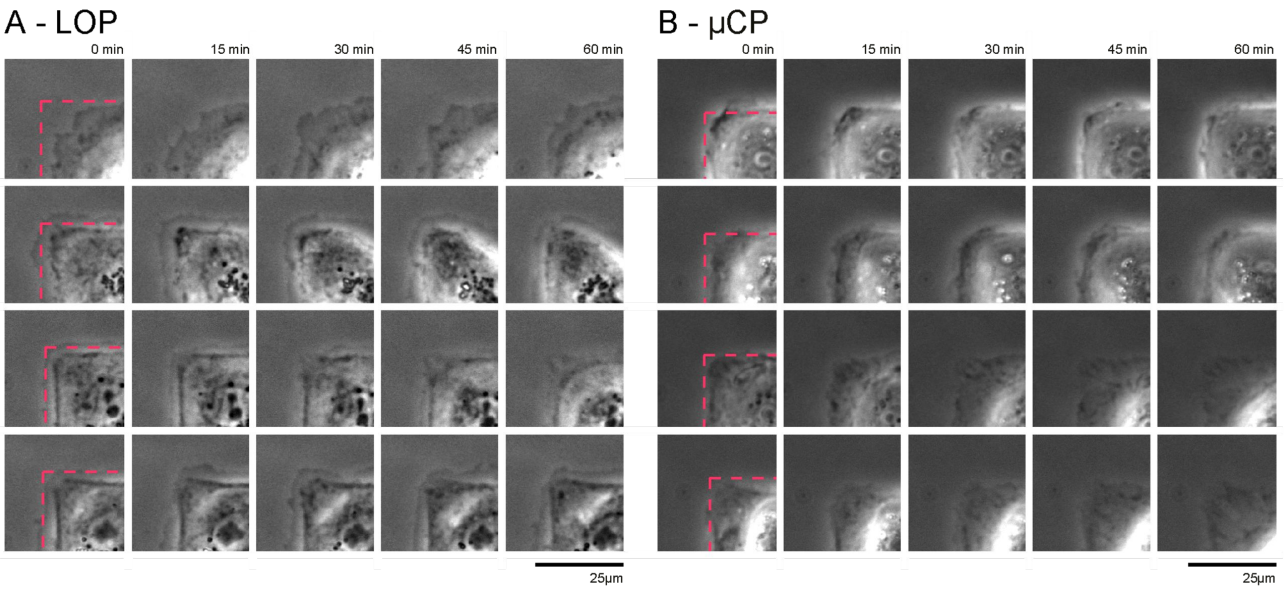
A - LOP
0 min
15 min
30 min
45 min
60 min
25µm
B - µCP
0 min
15 min
30 min
45 min
60 min
25µm

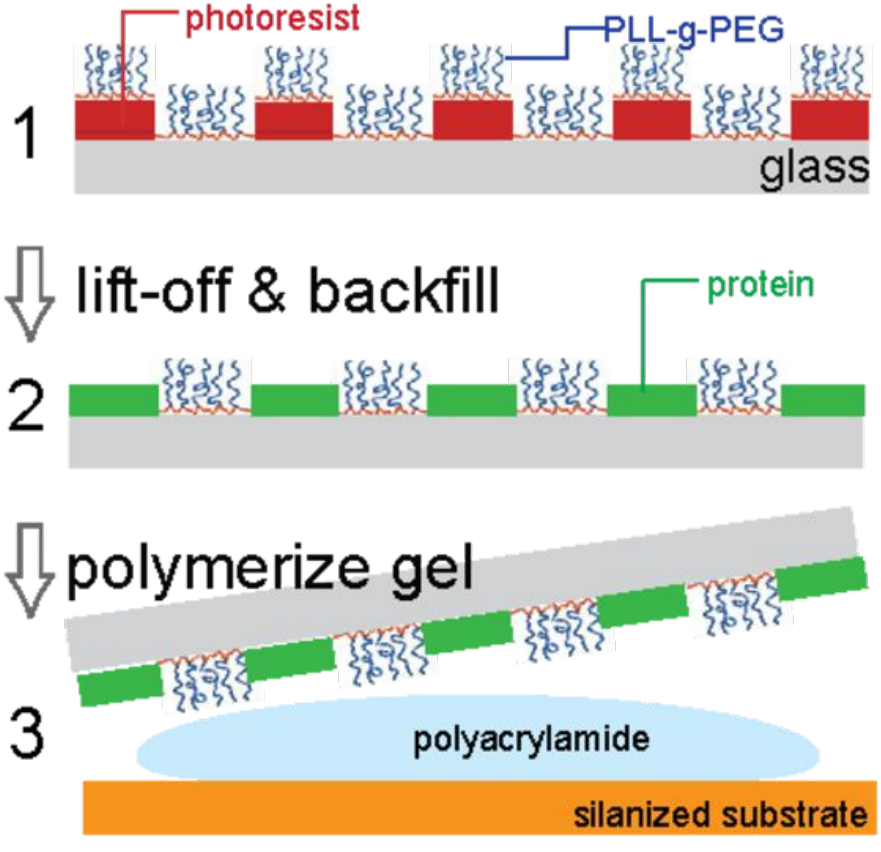

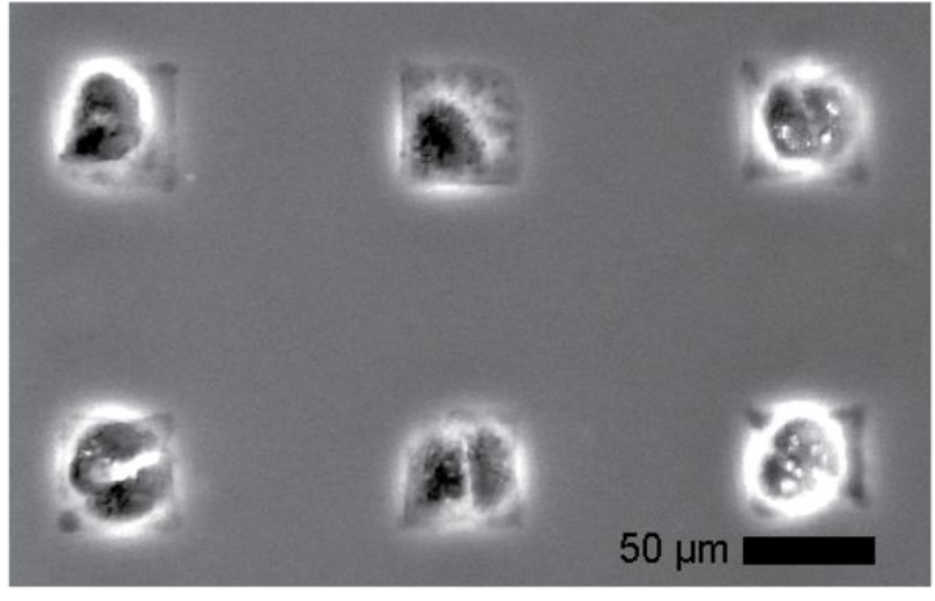

epithelial cell pairs cultured on patterned 10 kPa gel

Controlling cell shape on hydrogels using lift-off patterning

Jens Moeller*, Aleksandra K. Denisin*, Joo Yong Sim, Robin E. Wilson, Alexandre J.S. Ribeiro, Beth L. Pruitt
* authors contributed equally

Supplementary Information

SI Figure 1

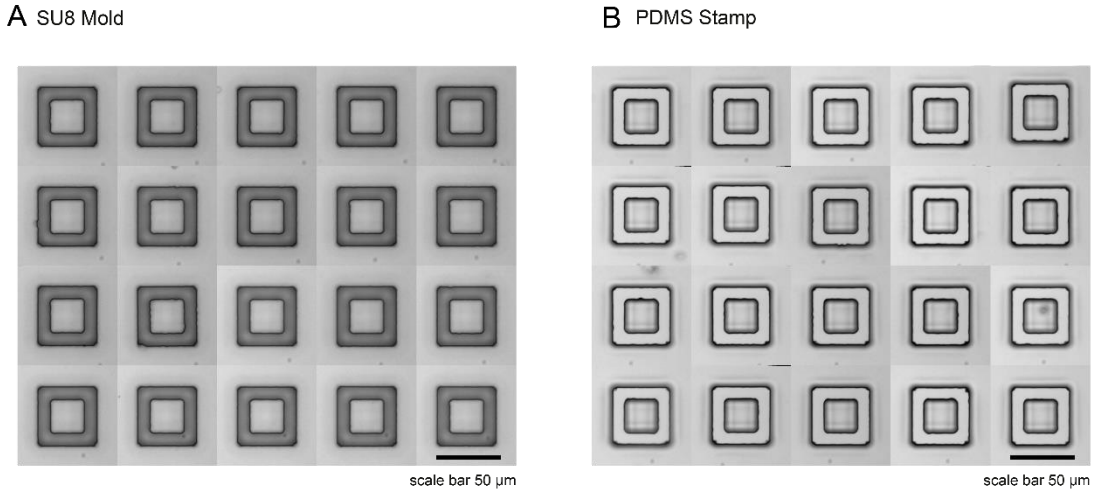

SI Figure 1 Overview of the SU8 master and PDMS stamps used for microcontact printing. The photolithography mold (A) and PDMS stamp cast from this mold (B) show rounded corners where the edges of the pattern meet, both in the inner and outer regions of the pattern. The height of the SU8 mold (~9 µm) may be limiting the pattern accuracy achievable with microcontact printing.

SI Movie 1 Single MDCK on LOP gel
Four separate time-lapse acquisitions (5 minute increments, time shown at upper left) of single MDCK cells on LOP-functionalized 25 kPa PAAm gels. Three channels are shown (gelatin for protein patterning, phase for cell outline, and LifeAct-GFP for actin structures). Scale bar is 45 µm wide.

SI Movie 2 Doublet MDCK cell pairs on LOP gel
Four separate time-lapse acquisitions (5 minute increments, time shown at upper left) doublet MDCK cell pairs on LOP-functionalized 25 kPa PAAm gels. Three channels are shown (gelatin for protein patterning, phase for cell outline, and LifeAct-GFP for actin structures). Scale bar is 45 µm wide.

SI Movie 3 Single MDCK on µCP gel
Four separate time-lapse acquisitions (5 minute increments, time shown at upper left) of single MDCK cells on µCP-functionalized 25 kPa PAAm gels. Three channels are shown (gelatin for protein patterning, phase for cell outline, and LifeAct-GFP for actin structures). Scale bar is 45 µm wide.

SI Movie 4 Doublet MDCK cell pairs on µCP gel
Four separate time-lapse acquisitions (5 minute increments, time shown at upper left) doublet MDCK cell pairs on µCP-functionalized 25 kPa PAAm gels. Three channels are shown (gelatin for protein patterning, phase for cell outline, and LifeAct-GFP for actin structures). Scale bar is 45 µm wide.

I. Lift-off Protocol

S1818 photolithography of coverslips

1. Wash the coverslips sequentially in acetone, isopropyl alcohol, and deionized water until all organic solvents are washed away. Carefully dry the coverslips with nitrogen gas.

2. Place coverslips on a 180°C hotplate for 5 min to complete drying process. When drying is finished store the coverslips again in individual boxes. Set the hotplate to 100°C and place a blank silicon wafer on top.

3. Align a chuck for spinning coverslips in the SU-8 spinner. Align a coverslip on the chuck and turn on the vacuum.

4. Select the following program parameters for the spinning protocol to achieve S1818 layer at 2µm thickness:
   5 seconds at 2000 RPM
   1 min 30 seconds at 4000 RPM

5. Use the transfer pipette to put ~0.5ml of S1818 onto the coverslip. Run the spin program.

6. When the program is finished, use a lint-free swab, dip in acetone and wipe around the edges of the coverslip to remove photoresist edge bead.

7. Bake at 100°C for 2 minutes. Transfer to individual box when baking is finished for cooling.

8. Expose each coverslip one at a time on the OAI system using a chrome mask of the design. Make sure that you put the coverslip on top of a silicon wafer to decrease back-scattering during exposure. You must achieve 40-50 mJ/cm^2 at 365 nm intensity for adequate exposure of the S1818. Determine exposure times based on calibration of the light source using a power meter.

9. Develop for 60 seconds in MF319 development solution. Rinse in deionized water, dry fully with nitrogen gas.

10. Verify the structures using a microscope.

Photoresist lift-off to fabricate protein patterned coverslips

1. Start with a S1818 photoresist structure on a clean glass slide (see S1818 photolithography protocol)

2. Clean suitable glass beakers (five of 25ml size; one 200ml size) with 2% Hellmanex solution overnight. Wash thoroughly with deionized water afterwards.

3. Fill the 25 ml beakers with N-Methyl-2-pyrrolidone (NMP), water and NMP / water mixture following this table of volume ratios:

Beaker	**1**	**2**	**3**	**4**	**5**
NMP fraction	1/3	-	1	1	1/2
Deionized water fraction	2/3	1	-	-	1/2

4. Incubate the S1818 structure with 100µg/ml PLL-g-PEG in PBS solution for 1 hour at room temperature. Place the droplet of PLL-g-PEG solution on top of the coverslip, do not use a method with inverting the slide on parafilm as this decreases transfer of the PLL-g-PEG to the glass.

5. Wash each sample three times with 1 ml of deionized water. Place each coverslip in a carrier for batch processing. Make sure you are aware of which side has the photoresist (it is best to face the coverslips all the same way with some kind of reference on the coverslip holder).

6. Begin the lift-off procedure by dipping the carrier of coverslips into beaker 1 for 20 seconds; agitate the coverslip carrier with tweezers.

7. Transfer the coverslip carrier into beaker 2 and leave for 10 seconds.

8. Transfer the coverslip carrier immediately into beaker 3 and sonicate for 1 minute.

9. Transfer the coverslip carrier into beaker 4 and sonicate for 5 minutes.

10. Transfer the coverslip carrier into beaker 5 and sonicate for 1 minute.

11. Transfer the coverslip carrier into a 200 ml beaker filled with distilled water. Agitate with a magnetic stir bar for 5 minutes.

12. Take each coverslip out of the carrier one by one and rinse three times with deionized water. Make sure you know which side of the coverslip was patterned. Dab the edge of each coverslip on a kimwipe to eliminate extra water. Avoid drying the coverslip.

13. Incubate each coverslip with 100 µg/ml protein solution for 1 hour at room temperature.

14. Wash sample three times with PBS and leave in PBS until use.

Microcontact printing of glass coverslips

1. Create a mold using photoresist on a silicon wafer. First, spin a uniform base layer (10 µm thickness) to increase adhesion of photoresist to the wafer and then use photolithography and a chrome mask (again with SU8 2010) to create the desired features. Follow Microchem manufacturer's suggestions for spinning, exposure dose, and baking parameters to get a 9 µm height feature layer.

2. Fabricate polydimethylsiloxane (PDMS) 'stamps' of features from a photoresist mold on a silicon wafer. Use 10:1 formulation of Sylgard 184.

3. Dice the PDMS wafer into 1 x 1 cm PDMS stamps containing the features of interest. Clean the PDMS stamps with an air gun and pipette a 100 µg/ml protein solution on top of the stamps. Spread the solution out to cover the stamp using a micropipette tip. Incubate the solution for an hour.

4. Aspirate the protein solution off the stamps with a pipette tip on vacuum tubing. Draw liquid off all of the sides without touching the patterned region. Use low nitrogen air flow to dry the stamps until all condensation disappears.

5. Use glass coverslips which have been cleaned overnight in 2% Hellmanex. Place the coverslip on a clean surface and then gently place your stamp straight down onto the coverslip. Avoid smearing and recentering if you already touched the PDMS to the glass surface. Lightly tap the stamp with tweezers to initiate contact spreading. Keep the coverslip and PDMS together for 5 minutes.

6. Using tweezers, firmly grasp the edge of the coverslip and lift it off the stamp surface (avoid smearing and loosing traction on the coverslip – proceed slowly). Place coverslip in a Petri dish with the patterned side up.

Polyacrylamide Gels Preparation on glass substrates

1. Prepare functionalized coverslips to bind polyacrylamide by mixing the bind-silane working solution (3 µl Bind-Silane, 50 µl acetic acid, and 50 µl 95% ethanol) and applying it to coverslips for 5 minutes. Then rinse the coverslips with ethanol and allow to dry in the dessicator.

2. Follow Table 1 below to determine the amount of acrylamide and bis-acrylamide (crosslinker) needed to create the desired stiffness gel. Pipette the water, acrylamide, and bis-acrylamide solutions into a centrifuge tube and take care not to introduce air bubbles while pipetting. Weigh out ammonium persulfate (APS) powder and create a 10% solution (w/v) using milliQ water.

Table 1: Polyacrylamide gel formulations used in this study

Stiffness (kPa)	**%T**	**%C**	**% Acryl.**	**% Bis.**	**Water (µl)**	**Acryl. (µl)**	**Bis. (µl)**	**APS**	**TEMED (µl)**
	Stock Concentration					**0.5 g/ml**	**0.025 g/ml**	**10%**	
25	10.25	2.44	10	0.25	694	200	100	5	1
10	10.10	0.99	10	0.1	754	200	40	5	1
5	5.15	2.91	5	0.15	834	100	60	5	1
%C = Crosslinker									
%T = Total Monomer (w/v)									
Acryl. = acrylamide									
Bis. = bisacrylamide									

3. Degas the mixture in the desiccator for 1 hour.

4. After degassing, take one tube of gel precursor at a time and add 5 µl of APS solution and 1 µl of TEMED (in that order). Mix well using the pipette tip but do not introduce bubbles.

5. Pipette the gel precursor mix onto the silanized coverslip and sandwich with protein patterned coverslip using 23 µl of solution for 18 mm round coverslips to yield a polyacrylamide gel 80 µm in height.

6. Wait for 30 min for polymerization at room temperature.

7. Following polymerization, immerse the gels in PBS overnight. Lift up the coverslip in PBS with a sharp tweezer when ready to use the gel surface for cell seeding or imaging of protein transfer. Store the gels in PBS in 4°C.

Comparisons between polyacrylamide pore size and gelatin protein molecular size

The volume of a gelatin molecule is smaller than the pore mesh size of all of the gel formulations used in our study and thus the molecule can diffuse into the matrix for any of the gels we used. Thus, when we visualize the gelatin using a fluorescent marker which is conjugated to it (Oregon Green), it must be attached to the gel as otherwise it would be free to diffuse in the surrounding medium and gel material.

Using relations by Holmes and Stellwagen (Holmes and Stellwagen, 1991) for polyacrylamide materials used for electrophoretic molecular sieving (Stellwagen, 1997), we note that our 25 kPa, 10 kPa, and 5 kPa gel formulations correspond to effective mean gel pore radius of 70 - 103 nm, 112 nm, and 100 nm, respectfully. These calculations were verified by measurements by Wen (Wen et al., 2014) and Hsu (Hsu and Cohen, 1984) of pore sizes ranging from 88 – 166 nm for similar gel formulations. Following methods outlined by Erikson (Erickson, 2009), we calculate each gelatin protein molecule (when modeled as a globular protein of 100 kDa) to have a volume of 121 nm^3, a minimum radius of 3.06 nm, and a Stokes radius of 12.57 nm given a diffusion coefficient of 1.75E-7 cm^2/s (Yoshimura et al., 2000).

References

Erickson, H.P. (2009). Size and shape of protein molecules at the nanometer level determined by sedimentation, gel filtration, and electron microscopy. Biol Proced Online *11*, 32-51.

Holmes, D.L., and Stellwagen, N.C. (1991). Estimation of polyacrylamide gel pore size from Ferguson plots of linear DNA fragments. II. Comparison of gels with different crosslinker concentrations, added agarose and added linear polyacrylamide. Electrophoresis *12*, 612-619.

Hsu, T.-P., and Cohen, C. (1984). Observations on the structure of a polyacrylamide gel from electron micrographs. Polymer *25*, 1419-1423.

Stellwagen, N.C. (1997). DNA mobility anomalies are determined primarily by polyacrylamide gel concentration, not gel pore size. Electrophoresis *18*, 34-44.

Wen, J.H., Vincent, L.G., Fuhrmann, A., Choi, Y.S., Hribar, K.C., Taylor-Weiner, H., Chen, S., and Engler, A.J. (2014). Interplay of matrix stiffness and protein tethering in stem cell differentiation. Nat Mater.

Yoshimura, K., Terashima, M., Hozan, D., Ebato, T., Nomura, Y., Ishii, Y., and Shirai, K. (2000). Physical properties of shark gelatin compared with pig gelatin. J Agric Food Chem *48*, 2023-2027.